Optimization of Vertical Screw Conveyor for Biomass Sampling: Influence of Pitch Geometry on Energy Dissipation and Material Integrity

Atchara Chaiya[1,2], Sarawut Pawako[2], Manat Okchol[2], Varut Sripaisan[2], Ninlawan Chaitanoo[1,2], Weeranut Intagun[3] and Autchara Junphong[1,2*]

[1]Research and Development Unit for Agricultural Materials and Bio-Energy Properties, Rajamangala University of Technology Lanna
128 Huay Kaew Road, Mueang, Chiang Mai, Thailand, 50300
[2] Department of Mechanical Engineering, Rajamangala University of Technology Lanna
128 Huay Kaew Road, Mueang, Chiang Mai, Thailand, 50300
[3]Department of Mechanical Engineering, Faculty of Engineering and Industrial Technology, Silpakorn University, Nakhon Pathom
6 Ratchamankha Nai Road, Phra Pathom Chedi Subdistrict, Mueang District, Nakhon Pathom Thailand, 73000
*Corresponding Author: Autchara11@rmutl.ac.th. Phone Number: 089-759-8846
Received: 31 December 2025, Revised: 16 March 2026, Accepted: 24 March 2026

Abstract
This study investigates the optimization of vertical screw conveyor design to enhance the efficiency and reliability of automated cassava sampling systems in agro-industrial processing. A comparative analysis was conducted between two screw configurations: Type B (P/D = 0.67) and Type C (P/D = 0.50), with varying screw diameters (0.11-0.20 m) and rotational speeds (56.78, 48.67, and 36.50 rpm for 18-, 21-, and 28-tooth gear sets, respectively) under controlled hydraulic operation (p = 152 bar, $Q_{oil} = 4.875\times10^{-4}$ m³/s, P_{in} = 7,410 W). The results indicate that over 99% of the hydraulic input power is theoretically dissipated as heat, based on the first-law energy balance. The Type B configuration, particularly at a diameter of 0.20 m and maximum rotational speed (56.78 rpm), demonstrated superior performance, achieving the lowest Specific Energy Consumption (SEC) of 23.25 kJ/kg, representing a 25.0% reduction in SEC and a 33.4% gain in useful mechanical work output (P_{out} : 14.07 vs. 10.55 W) over Type C. Furthermore, the wider pitch of Type B effectively mitigates material compaction and reduces cumulative frictional stress during transport, preserving the physical integrity of cassava chips (bulk density: 496.4 ± 62.4 kg/m³; moisture content: 13.5 ± 0.5% w.b.). The study concludes that the Type B configuration is the optimal design for maximizing flow stability and minimizing energy loss while satisfying quality assurance requirements.
Keywords: Vertical Screw Conveyor, Specific Energy Consumption (SEC), Energy Dissipation, Sampling Integrity, Cassava sampling

1. Introduction

In agro-industrial cassava processing, bulk solids handling is a critical unit operation directly influencing process efficiency and product quality. Cassava chips exhibit high physical property variability, requiring a robust sampling system to ensure quality assurance (QA) accuracy under the Process Analytical Technology (PAT) framework; any sampling bias leads to significant errors in moisture content and starch yield estimation [1]. The core engineering challenge in vertical screw-based sampling units is the complex momentum transfer and hydrodynamics of non-uniform biomass. As material is conveyed vertically against gravity, internal and wall friction generate resistance, causing momentum loss, slippage, and unstable mass flux. According to Roberts [2] and Bridgwater [3], volumetric efficiency is highly sensitive to pitch-to-diameter ratio; inefficient geometry induces flow discontinuities that are a

primary source of sampling bias in automated industrial systems [4],[5].

Process safety presents an additional engineering challenge. Frictional heat dissipation - governed by transport phenomena principles [6] - can cause hazardous heat accumulation in short-pitch configurations. Recurrent clogging represents states of zero momentum transfer where all input energy converts to thermal energy, creating localized ignition sources. Combined with combustible fines generated through particle attrition, this significantly elevates the risk of dust explosions under the Dust Explosion Pentagon framework [7],[8].

Despite extensive theoretical and computational work - including the granular rheology framework of Roberts [2], DEM-based conveying models of Owen and Cleary [9], biomass-specific feeding studies by Rackl and Günthner [10], and recent DEM and CFD studies [11-13] - a critical gap remains: no experimental data simultaneously characterizes energy partitioning and material integrity as a direct function of P/D ratio for fragile agricultural feedstocks under vertical hydraulic conveying. This study addresses that gap directly by optimizing the vertical sampling unit for cassava chips through analysis of screw geometry, flow stability, and energy dissipation - identifying an optimal configuration that preserves sampling integrity, minimizes biochemical degradation risk, and supports scale-up of automated sampling in large-scale biorefineries.

2. Materials and Methods

2.1 Feedstock Characterization

The feedstock utilized in this study was commercial-grade cassava chips (Figure 1a), characterized by high morphological heterogeneity and an irregular, fibrous structure (Figure 1b). From a process engineering standpoint, these physical attributes govern the interparticle momentum transfer and the resulting flowability of the bulk solid [1], [3].

The average bulk density (ρ_b) was determined to be 496.4 ± 62.4 kg/m³ (0.4964 ± 0.0624 g/cm³). The moisture content (MC) was strictly maintained at 13.5 ± 0.5% (wet basis) to simulate standard industrial conditions. This parameter is critical as it influences the interfacial friction and cohesive forces, which directly affect the internal shear stress (τ) distribution and the potential for mechanical interlocking within the screw flight [2], [14].

a) b) c)

Figure 1 Physical Properties and Conveying Behavior of Cassava Chips

a) Harvested cassava roots from the field.

b) A representative cassava chip (length: 70-100 mm) with a 20 mm scale bar (approximate, based on chip reference dimensions).

c) The screw conveyor-based automatic sampling system operating during

2.2 Experimental Setup and Geometric Boundary Conditions

The automated sampling unit (Figure 1c) serves as the control volume for this investigation. The boundary conditions and operational constraints were defined by the interaction between the screw geometry and the drive system. The experimental design focused on two distinct screw configurations, as summarized in the design matrix in Table 1.

Table 1 Experimental Design Matrix and Geometric Boundary Conditions of the Vertical Screw Sampling System

Screw Configuration Type	Pitch-to-Diameter Ratio (P/D)	Drive Ratio (Gear Teeth Count, n_2)	Screw Diameter Range (D), [m]
Type B	2/3	18, 21, 28	0.11 – 0.20
Type C	1/2	18, 21, 28	0.11 – 0.20

The selection of Type B (P/D = 0.67) and Type C (P/D = 0.50) geometries (Figures 2 and 3) enables evaluation of how pitch compression ratio and gear-regulated rotational speed affect transport

phenomena and energy dissipation. These P/D values represent the practical manufacturing extremes within D = 0.11- 0.20 m using standard CNC fabrication, establishing the performance envelope within which intermediate configurations (e.g., 0.55–0.65) must operate; their investigation is identified as a priority for future work.

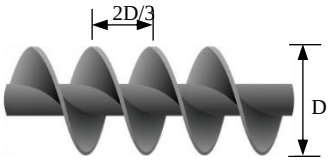

Figure 2 Full-pitch screw with 2D/3 pitch length.

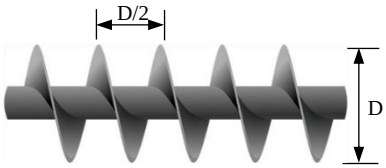

Figure 3 Full-pitch screw with D/2 pitch length.

The experimental configuration replicates the hydraulic drive setup at the Betagro cassava processing facility (Lopburi Province, Thailand), ensuring direct industrial applicability without system redesign. Alternative technologies were excluded on technical grounds: belt conveyors cannot achieve the required vertical transport angle under cassava chip bulk density and moisture conditions [1], and pneumatic conveying induces particle fragmentation and moisture loss that compromise sampling integrity [3]. The hydraulic screw conveyor therefore uniquely satisfies all operational constraints - vertical transport, chip morphology preservation, and process infrastructure compatibility. Screw diameters (D) ranged from 0.11 to 0.20 m, and the instrumentation setup (Figure 4) enabled real-time acquisition of hydraulic pressure (p), oil flow rate (Q oil), and mass flow rate ($\dot{m}$) for comprehensive transport analysis [5].

Both Type B and Type C flights were fabricated from the same mild steel batch under identical CNC specifications; flight thickness and surface roughness (Ra) therefore constitute controlled constants, and any difference in η_v or SEC is attributable exclusively to P/D ratio. Profilometer measurement of *Ra* is recommended as a standard protocol when comparing flights of different materials in future studies.

The screw shaft speed (N) was set by a chain-and-sprocket drive governed by Equation (1):

$$N = N_{motor} \times (n_1 / n_2) \quad (1)$$

where N_{motor} = 73 rpm (hydraulic motor output speed), n_1 = 14 teeth (fixed driving sprocket), n_2 = interchangeable driven sprocket (18, 21, or 28 teeth). The calculated shaft speeds ($N_{motor} \times n_1/n_2$ = 73 × 14/18 = 56.78, 73 × 14/21 = 48.67, 73 × 14/28 = 36.50 rpm) match the directly measured shaft speeds to within ±0.01 rpm (CV < 0.004%), confirming stable hydraulic drive output across all gear settings.

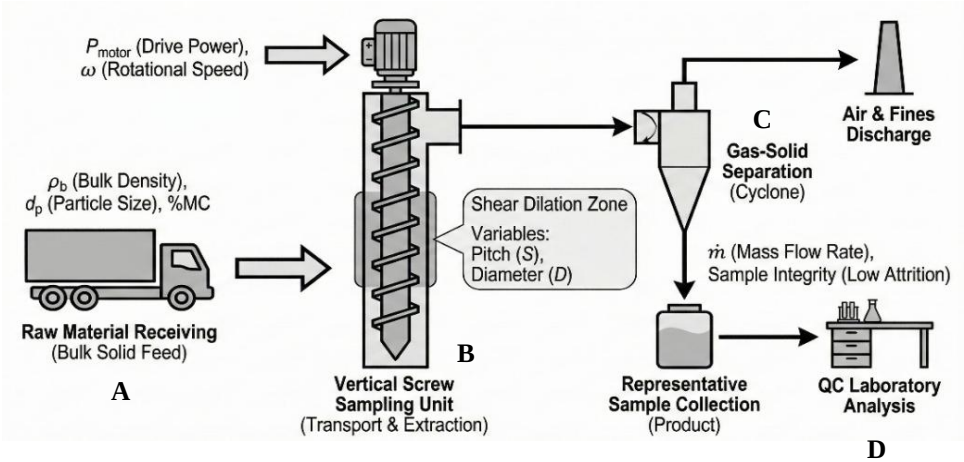

Figure 4 Process Flow Diagram of Cassava Chip Sampling Unit Operation.

2.3 Theoretical Framework and Governing Equations

To ensure scientific rigor, the unit operation was analyzed through the lens of conservation laws and dimensionless transport parameters.

2.3.1 Momentum Transport and Mass Flux Stability

The efficiency of mass transport was quantified via the Volumetric Efficiency (η_v) shown in Equations (2) and (3), which serves as a dimensionless indicator of the stability of the Mass Flux and the degree of momentum loss due to material slippage [15]:

$$\eta_v = \frac{\dot{m}_{actual}}{\dot{m}_{theoretical}} \quad (2)$$

$$\eta_v = \frac{\dot{m}_{actual}}{\rho_b \times A \times P \times N} \quad (3)$$

where A is the effective cross-sectional area, P is the screw pitch, and N is the rotational speed. A significant deviation of η_v from unity indicates inefficient momentum coupling between the screw flight and the material bed, often caused by internal shear losses [2], [10].

2.3.2 Conservation of Energy and Dissipative Heat Generation

Applying the first law of thermodynamics to the sampling unit, the total hydraulic power input (P_{in} or P_{total}) is partitioned into productive potential energy and dissipative losses. The fundamental energy balance for this vertical transport operation is defined as Equation (4):

$$P_{total} = P_{potential} + Q_{gen} \quad (4)$$

Where $P_{potential}$ represents the energy rate required for the vertical displacement of the material ($\dot{m}gh$), and Q_{gen} represents the rate of dissipative heat generation primarily arising from inter-particle and wall friction. The heat generation rate is further derived as Equation (5).

$$Q_{gen} = (p \times Q_{oil}) - (\dot{m}gh) \quad (5)$$

Where

p = The hydraulic pressure (Pa or kg-m/s^2)
Q_{oil} = The oil flow rate (m^3/s)
$\dot{m}$ = Mass flow rate (kg/s)
g = The gravitational acceleration (m/s^2)
h = The vertical transport heigh (m)

Evaluating Q_{gen} is a critical step in assessing Process Safety, as excessive heat accumulation can lead to Thermal Degradation of the starch or serve as a potential Ignition Source in dust-prone environments [7], [8].

To evaluate the process efficiency independent of throughput capacity, the specific energy consumption (SEC) was determined. SEC serves as a standardized metric to compare the energy cost per unit mass of material transport as Equation (6):

$$SEC\ (kJ/kg) = \frac{P_{total}}{\dot{m}} \quad (6)$$

where P_{total} is the total power input (kW) and $\dot{m}$ is the mass flow rate (kg/s). A surge in SEC values indicates a transition from efficient conveying to a high-friction regime, where energy is wasted on mechanical grinding rather than transport [7].

2.4 Evaluation of Sampling Integrity and Attrition Kinetics

The preservation of the feedstock's physicochemical properties, defined as sampling integrity, was evaluated through particle attrition analysis. According to the principle of mass conservation, mechanical stress induces size degradation, leading to fines generation, which is quantified as a source of sampling bias [1], [16]. The interaction between energy dissipation (Q_{gen}) and mechanical interlocking was analyzed to establish the operational limits, ensuring that the extracted samples accurately reflect the feedstock quality without induced thermal or mechanical degradation.

2.5 Statistical Analysis

One-way analysis of variance (ANOVA) was performed to compare mass flow rate, volumetric efficiency (η_v), and SEC between Type B and Type C configurations across the three gear speed conditions (18-, 21-, and 28-tooth gear). Post-hoc pairwise comparisons were conducted using Tukey's HSD test. All analyses were performed at $\alpha = 0.05$. Statistically significant differences between Type B and Type C were confirmed for all primary performance variables ($p < 0.05$).

3. Results and Discussions

3.1 Operational Baseline and Process Failure Analysis

A longitudinal retrospective analysis covering the operational period from May to April was conducted to diagnose the baseline performance of the existing screw conveyor-based sampling system. The empirical data revealed a consistent pattern of mechanical failure, characterized by an average of three clogging incidents per month, which resulted in a cumulative downtime of approximately 126 minutes per month. Notably, the peak operational instability was recorded in September, when the downtime escalated to nearly 240 minutes.

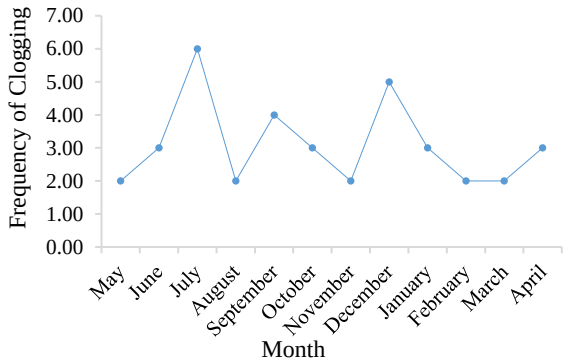

Figure 5 Monthly frequency of clogging in the cassava chip screw sampling system.

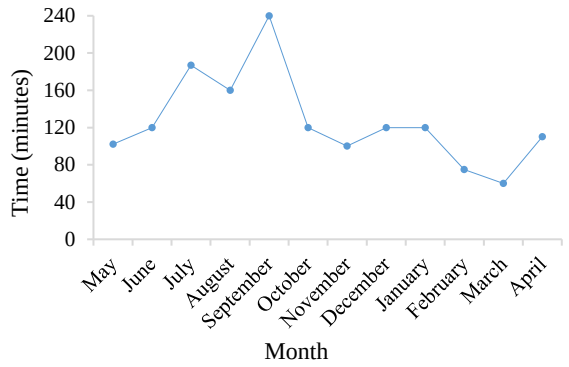

Figure 6 Comparison of monthly repair time required to resolve clogging issues in the cassava chip screw sampling system.

These blockage episodes, as illustrated in Figure 5, are not merely operational disruptions but critical indicators of momentum stagnation. In the context of granular rheology, these recurring stoppages signify a transition from a dynamic flow regime to a static "jamming state," where the motive torque of the drive system is overwhelmed by the internal shear stress of the cassava chips. This phenomenon aligns with the mechanical interlocking hypotheses for fibrous bulk solids described by Roberts [2].

Furthermore, Figure 6 quantifies the repair duration associated with these failures. From a process safety perspective, these extended downtimes represent periods of dangerous thermal accumulation. When the screw jams, the input kinetic energy is instantaneously converted into frictional heat at the blockage point. According to the energy balance principle in Equation (4), this creates localized "hot spots" that can approach the minimum ignition temperature of dry biomass dust. This finding underscores a severe safety hazard, as highlighted by Amyotte & Eckhoff [7] in the *Dust Explosion Pentagon* framework, thereby necessitating a geometric redesign to mitigate thermal risks.

3.2 Analysis of Momentum Transport and Volumetric Efficiency

This section evaluates the critical factors influencing the vertical transport of cassava chips within the lift system. The analysis integrates the geometric design of the screw flights with kinematic operational parameters to determine their collective impact on momentum transfer and the resulting flow regimes.

3.2.1 Geometric Boundary Conditions

To interpret the transport mechanisms governing system performance, the geometric boundary conditions of the two screw configurations were evaluated, as illustrated in Figure 7. The analysis reveals a distinct hydrodynamic divergence between the two profiles. Type B, characterized by an extended pitch-to-diameter ratio (P = 2D/3), creates a larger control volume between flights. This geometry theoretically minimizes the granular packing fraction (ϕ), allowing the fibrous cassava chips to align naturally with the helical flight angle. Consequently, this configuration promotes a "plug flow regime," where the material is transported as a cohesive block with minimal internal shear, thereby maximizing the efficiency of momentum transfer.

In sharp contrast, the compressed profile of Type C (P = D/2) significantly restricts the available volumetric capacity per revolution. From

a granular rheology perspective, this geometric constraint increases the "arching effect" probability, forcing the biomass bed into a "compacted/shear regime." In this state, the dominant mechanical force shifts from vertical lift to lateral wall friction, explaining the theoretical tendency for energy dissipation and flow instability observed in restricted-pitch designs.

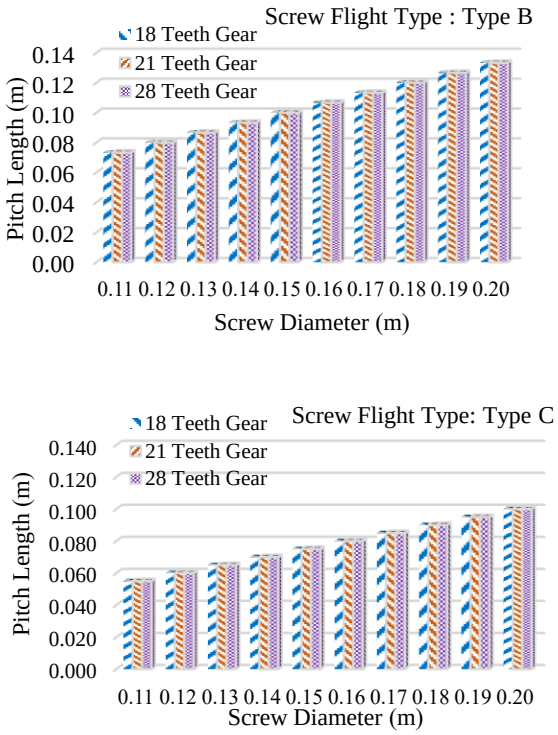

Figure 7 Comparison of screw flight diameter (D) and pitch length for Type B and Type C.

3.2.2 Kinematic Stability Validation

The stability of the drive system was verified to ensure that the screw rotational speed (N) remained independent of the geometric variables. Figure 8 delineates the operational parameters governed by the drive system setup. The rotational speed (N) was determined solely by the selected gear ratio and remained independent of the screw diameter (D). As illustrated, the 18-tooth gear set provided the highest rotational speed (~57 rpm), exceeding the 50 rpm reference line, thereby generating the highest shear rate conditions for the study. Conversely, the 28-tooth gear set yielded the lowest speed (~36 rpm). This confirmation of constant speed across varying diameters ensures that any observed differences in mass flow rate (discussed in the next section) are attributable to screw geometry and diameter effects, rather than kinematic fluctuations.

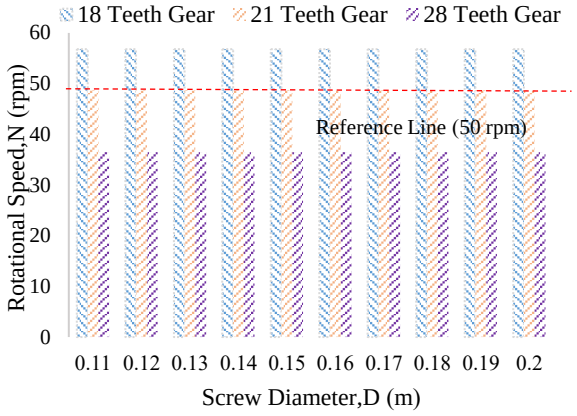

Figure 8 Relationship between screw flight diameter (D) and rotational speed for Type B and Type C configurations.

In Equation (1) (Section 2.2), the back-calculated chain-interface speed ($N_{motor} \times n_1 = 73 \times 14 = 1{,}022$ rpm, CV < 0.004%) confirms stable hydraulic drive output across all gear settings, validating that observed performance differences between Type B and Type C are attributable solely to P/D geometry.

3.2.3 Mass Flux Characteristics and Regime Transition

With the kinematic stability confirmed, the mass transport performance of the two screw profiles was evaluated against the pilot-scale requirement of 11.36 kg/cycle. The comparison in Figure 9 is conducted at the maximum rotational speed (18-tooth gear) to clearly demonstrate the divergence in transport efficiency between the two geometric profiles under high-load conditions.

As illustrated in Figure 9, the data demonstrates the superior capability of the Type B configuration. The system consistently achieved or exceeded the target capacity threshold (indicated by the red dashed line) at screw diameters of $D \geq 0.14$ m. This high performance validates the theoretical assumption that the extended pitch geometry (P = 2D/3) reduces internal friction and promotes a "Plug Flow Regime," which maximizes the efficiency of momentum transfer from the screw to the cassava chips.

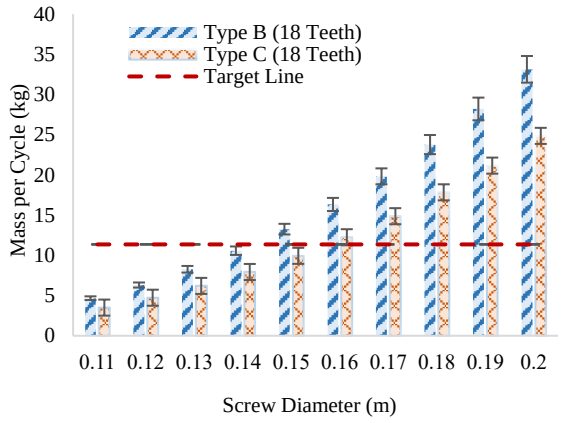

Figure 9 Comparison of conveying capacity per cycle between Type B and Type C screw flights at maximum rotational speed (18-tooth gear).

In contrast, the limitations of the restricted geometry are evident in the performance of Type C. To meet the same 11.36 kg throughput, this configuration required significantly larger diameters ($D \geq 0.16$ m) even at the maximum rotational speed. This performance lag indicates a transition into a "high-slip regime," where the restricted pitch ($P = D/2$) causes the material to rotate with the screw rather than advancing vertically. Although the narrow error bars for Type C suggest high operational stability, this is achieved at the cost of momentum decoupling, necessitating higher kinetic energy to overcome the increased frictional resistance within the confined pitch space.

The experimental analysis illustrated in Figures 10 and 11 reveals that the volumetric efficiency (η_v) of the system consistently remains below 40%. In the context of bulk solids handling engineering, this performance is theoretically consistent with the principles established by Roberts [2], which state that agricultural materials with irregular geometries and high internal friction, such as cassava chips, exhibit a low filling degree within the screw flights. This phenomenon is primarily attributed to material interlocking, where the non-spherical nature of the chips creates substantial internal voids during transport, preventing the material from fully occupying the screw's theoretical geometric volume.

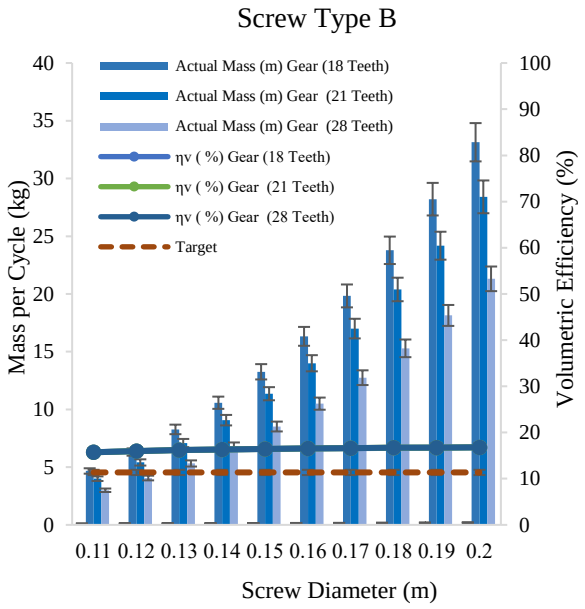

Figure 10 Comparative analysis of mass flow rates and volumetric efficiencies for the Type B screw (P/D = 0.67) across various screw diameters and gear configurations.

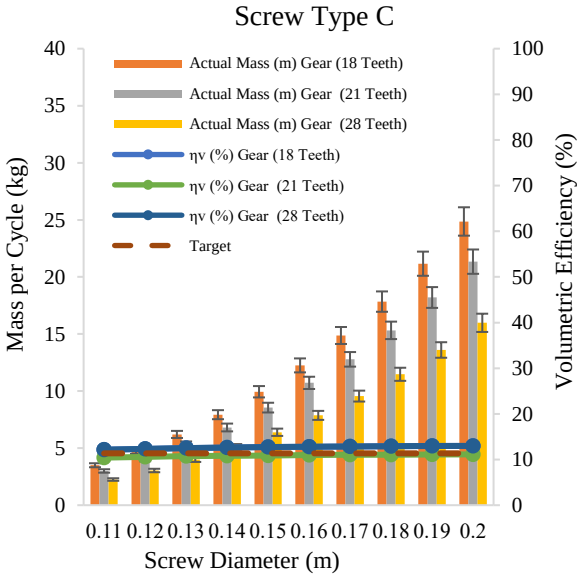

Figure 11 Comparative analysis of mass flow rates and volumetric efficiencies for the Type C screw (P/D = 0.5) across various screw diameters and gear configurations.

Furthermore, the observed decline in efficiency within the Type C screw (P/D = 0.5) compared to the Type B screw (P/D = 0.67) can be elucidated through the theory of vortex flow and internal shear resistance as proposed by Woodcock and Mason [16]. The restricted pitch of Type C

induces higher internal shear and circumferential slippage (momentum decoupling), further intensified at elevated rotational speeds [16].

Despite the relatively low absolute efficiency values, the comparative data underscores the superior performance of the Type B design in maintaining a stable volumetric efficiency across all tested diameters. This validates the geometric optimization hypothesis, asserting that an optimized pitch-to-diameter ratio promotes a more effective plug flow regime and mitigates material compaction. Consequently, the Type B configuration demonstrates the capacity to achieve the design target of 11.36 kg per cycle even under challenging rheological conditions, aligning with agricultural machinery design standards that prioritize operational reliability over theoretical maximum capacity [17].

3.2.4 Speed-Dependent Mass Transport Response and Pitch Geometry Influence

The experimental results illustrated in Figure 12 demonstrate a strong linear correlation between rotational speed and mass flow rate per cycle across all tested configurations ($R^2 > 0.98$). At a constant screw diameter, increasing the rotational speed from 36.50 to 56.78 rpm leads to a proportional rise in mass transport capacity. However, the rate of this increase-represented by the slope of the regression lines-is significantly governed by the pitch-to-diameter (P/D) ratio. For instance, at D = 0.16 m (Figure 12b), the Type B configuration (P/D = 0.67) exhibits a steeper gradient (m = 0.144) compared to the Type C configuration (P/D = 0.50, m = 0.113), indicating that a larger pitch enhances the system's sensitivity to rotational input.

From a fluid-solid dynamics perspective, the divergence between Type B and Type C geometries suggests a transition in flow efficiency. The Type B configuration facilitates a more effective axial displacement per revolution, maximizing the axial velocity of the cassava chips. In contrast, the restricted geometry of Type C (P/D = 0.50) appears to induce a "high-slip" regime, particularly at elevated speeds. In this state, a significant portion of the kinetic energy is dissipated through material rotation (tumbling) within the screw flights rather than productive forward advancement. This observation aligns with the findings of Owen and Cleary [9], which suggest that optimal pitch lengths are crucial to reducing internal granular friction and maintaining flow stability.

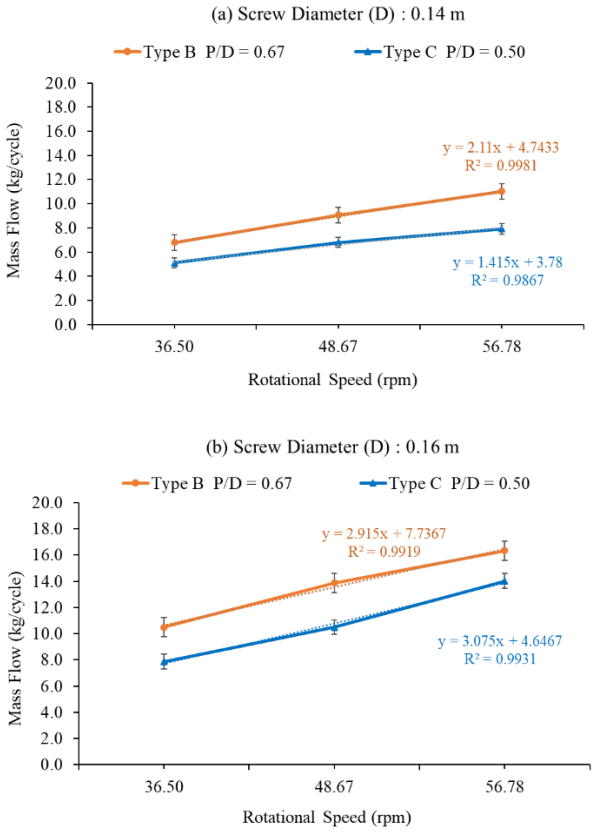

Figure 12 Effect of rotational speed on mass flow rate per cycle for Type B (P/D = 0.67) and Type C (P/D = 0.50) configurations at: (a) D = 0.14 m and (b) D = 0.16 m.

The correlation analysis further identifies the critical role of screw diameter in achieving performance targets. As shown in Figure 12a (D = 0.14 m), neither configuration consistently achieves the pilot-scale target of 11.36 kg/cycle, with Type B reaching a plateau near 11.0 kg/cycle. However, by increasing the diameter to 0.16 m (Figure 12b), the Type B configuration successfully surpasses the 11.36 kg/cycle threshold once the rotational speed exceeds approximately 49 rpm. Conversely, Type C fails to reach this target even at the maximum diameter and speed, confirming that momentum decoupling

occurs when the P/D ratio is too low to overcome the internal shear of fibrous granular materials.

Ultimately, these results validate the "plug flow" characteristics of the Type B design, where the material moves as a coherent mass with minimal internal velocity gradients. The high R^2 values (0.9867-0.9981) confirm that the mass transport remains highly predictable within the tested range, providing reliable empirical coefficients for engineering specifications. These findings support the principles established by Roberts [2] regarding the critical helix angle required to optimize volumetric efficiency. The study concludes that for cassava chip transport, a P/D ratio of 0.67 combined with a 0.16 m diameter is essential to ensure consistent throughput that meets industrial requirements.

3.3 Energy Dissipation characteristics and their Impact on Sampling Integrity

The analysis of energy partitioning was conducted under constant operating conditions (p = 152 bar, $Q_{oil} = 4.875\times10^{-4}$ m³/s, t = 104 s, h = 4.5 m). The distribution of total input power (P_{in}) into effective mechanical work (P_{out}) and heat dissipation (Q_{gen}) is shown in Figure 13.

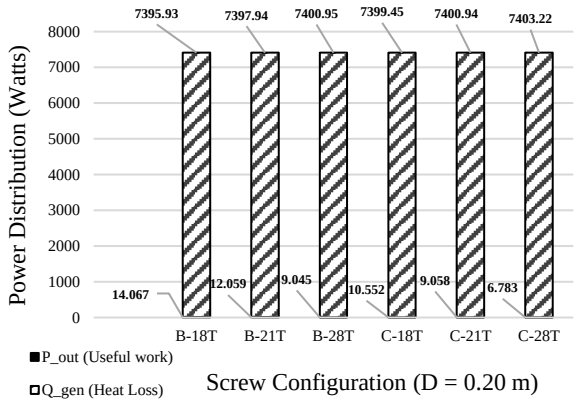

Figure 13 Distribution of total input power (P_{in}) into effective mechanical work (P_{out}}) and heat dissipation (Q_{gen}) for the hydraulic vertical screw conveyor system.

Over 99% of hydraulic input power is theoretically dissipated as heat (Q gen) - a theoretical upper-bound estimate from the first-law energy balance (Equation 4), as no direct calorimetric measurement was performed. This is consistent with vertical screw conveying theory [16], which holds that most input energy overcomes internal shear resistance, wall friction, and vortex motion rather than elevating the bulk load.

Although mechanical efficiency is low across all configurations, significant differences exist between geometries. Type C (P = 0.5D) consistently exhibited higher SEC and greater Q gen than Type B, attributable to its restricted pitch inducing higher internal compaction and frictional drag between chips and casing. The frictional energy (Q_{gen}) is transferred to the material as mechanical stress and thermal energy, increasing cumulative stress on individual chips during transport. Such elevated stress raises the risk of morphological change and may alter chip bulk density, introducing sampling bias where sample characteristics no longer accurately represent the bulk load.

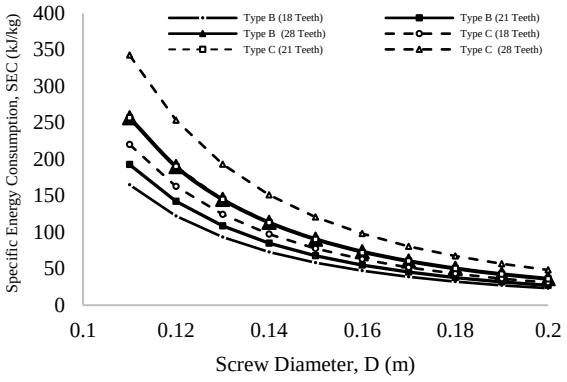

Figure 14 Effect of screw diameter on Specific Energy Consumption (SEC) for screw configurations Type B and Type C at various rotational speeds.

In contrast, Type B (P = 0.67D) demonstrated superior performance. As shown in Figure 14, Type B achieved the lowest SEC of 23.25 kJ/kg at D = 0.20 m and maximum rotational speed (18-tooth gear). Its wider pitch reduces internal compaction and frictional losses, lowering cumulative mechanical stress per unit mass conveyed and better preserving chip morphology and sampling representativeness.

According to the quantitative research in Table 2, the Type B arrangement reduces specific energy consumption (SEC) by 25.0% while increasing usable mechanical work (P_{out}) by 33.4% compared to Type C. The significant improvements confirm that the modified pitch-to-diameter ratio (P/D = 0.67) efficiently reduces material jamming and decreases internal friction. Despite the minimal percentage change in heat loss (Q_{gen}) of 0.05% attributed to the predominance of input power, the significant increase in mechanical output (Pout) demonstrates that Type B transfers available energy into material movement with greater efficiency. This efficiency lowers energy expenditures per unit mass and reduces mechanical stress on cassava roots, preserving the samples' physical integrity and allowing for reliable quality assessment.

Type B reduces SEC by 25.0% and increases useful mechanical work output (P out) by 33.4% relative to Type C (Table 2). The near-identical Q_{gen} values (7,395.93 vs. 7,399.45 W; Δ = 3.52 W, 0.05%) confirm that both configurations dissipated equivalent frictional heat and neither imposed thermally damaging conditions on the chips. The 25.0% reduction in SEC indicates lower cumulative mechanical stress per unit mass conveyed, directly supporting better preservation of chip morphology and sampling representativeness. This study involves conveying only - no grinding or size-reduction was performed; Q_{gen} reflects chip-to-flight wall friction and inter-chip friction during vertical transport, not particle size reduction.

Table 2 Comparison of optimal performance parameters between Type B and Type C configurations at maximum rotational speed (18-tooth gear) and 0.20 m diameter.

Parameter	Type B (P/D = 0.67)	Type C (P/D = 0.50)	% Improvement
Heat Loss (Q_{gen})	7,395.93 W	7,399.45 W	0.05%
Specific Energy (SEC)	23.25 kJ/kg	31.00 kJ/kg	25.0%
Useful Work (P_{out})	14.07 W	10.55 W	33.4%

As shown in Table 3, the SEC of 23.25 kJ/kg achieved by Type B exceeds the 4.14–10.6 kJ/kg reported by Rackl and Günthner [10] for horizontal wood chip feeding, consistent with the higher energy demand of vertical transport against gravity and vortex motion [16]. Yuan et al. [11] demonstrated via DEM simulation that pitch geometry governs vertical conveying capacity, and Hamed et al. [13] established material-geometry interactions as principal determinants of SEC (0.5-2.0 kJ/kg for horizontal Douglas fir at 48 rpm). Collectively, these benchmarks confirm that P/D optimization alone yields statistically significant performance gains ($P \leq 0.008$) for fibrous biomass in vertical conveying applications.

Table 3 Comparison of key performance indicators with published literature on screw conveying of agricultural biomass.

Parameter	This study Type B (P/D=0.67)	This study Type C (P/D=0.50)	Rackl & Günthner [11]	Yuan et al. [15]	Hamed et al. [17]
SEC (kJ/kg)	23.25	31.00	4.14 – 10.6[a]	-	0.5–2.0[b]
η_v (%)	16.34	12.02	-	-	-
Mass flow	8.82 kg/cycle	6.61 kg/cycle	quasi-static	~250 t/h	60–75 kg/h
Material	Cassava chips	Cassava chips	Wood chips (spruce)	Soybean	Douglas fir
P/D ratio	0.67	0.50	1.17–1.33	N/A (variable)	1.0
Conveyor type	Vertical hydraulic	Vertical hydraulic	Horizontal	Vertical	Horizontal

[a] Based on effective power consumption (E_{eff}) reported by Rackl & Günthner [10], Fig. 14
[b] Specific energy at 48 rpm, from Hamed et al. [13], Fig. 6c

Table 4 One-way ANOVA and Tukey's HSD post-hoc results (Type B vs. Type C; n = 9 per group; α = 0.05). **P < 0.01.

Variable	D(m)	Type B (P/D=0.67) Mean ± SD	Type C (P/D=0.50) Mean ± SD	$F_{(1,16)}$	P-value	Sig.	Tukey HSD
Mass flow rate (kg/cycle)	0.14	8.817 ± 1.647	6.609 ± 1.232	10.369	0.005	**	A vs B
η_v (%)	0.14	16.340 ± 0.009	12.023 ± 0.903	205.852	< 0.001	**	A vs B
SEC (kJ/kg)	0.20	28.846 ± 5.738	38.447 ± 7.665	9.049	0.008	**	A vs B

3.4 Statistical Analysis of Performance Differences Between Screw Configurations

One-way analysis of variance (ANOVA) was performed using Minitab 19 (Minitab LLC, State College, PA, USA) to determine whether statistically significant differences existed between Type B (P/D = 0.67) and Type C (P/D = 0.50) for three primary response variables: mass flow rate, volumetric efficiency (η_v), and specific energy consumption (SEC). Each group comprised n = 9 observations (three gear speeds × three replicates). Levene's test confirmed equal variances for all variables (all P > 0.05; α = 0.05). Complete results are presented in Table 4.

ANOVA results are summarized in Table 4. Mass flow rate (D = 0.14 m) differed significantly between configurations [F(1,16) = 10.369, P = 0.005], with Type B: 8.817 ± 1.647 kg/cycle vs. Type C: 6.609 ± 1.232 kg/cycle (Tukey HSD 95% CI [0.754, 3.661]). Volumetric efficiency showed the largest effect [F(1,16) = 205.852, P < 0.001]: Type B 16.340 ± 0.009% vs. Type C 12.023 ± 0.903% (95% CI [3.679, 4.954]). SEC (D = 0.20 m) also differed significantly [$F_{(1,16)}$ = 9.049, P = 0.008]: Type B 28.846 ± 5.738 vs. Type C 38.447 ± 7.665 kJ/kg (95% CI [-16.367, -2.835]). All three variables showed statistically significant differences (P ≤0.008), confirming that the performance advantages of Type B are not attributable to random variation.

4. Conclusions

This study successfully identifies the optimal vertical screw conveyor design for enhancing the efficiency of automated cassava sampling systems. Through a rigorous comparative analysis between Type B (P/D = 0.67) and Type C (P/D = 0.50) configurations, the investigation reveals that increasing the screw pitch ratio significantly improves energy performance. Specifically, the Type B configuration operating with a 0.20 m diameter and at maximum rotational speed achieved the lowest Specific Energy Consumption (SEC) of 23.25 kJ/kg. This corresponds to a 25.0% improvement in energy efficiency compared to the Type C configuration under identical conditions, confirming that the optimized pitch geometry effectively minimizes the power required per unit mass of transport.

A critical examination of energy partitioning further elucidates the mechanism behind this performance enhancement. While the analysis confirms that over 99% of the hydraulic input power is theoretically dissipated as heat - a theoretical upper-bound estimate from the first-law energy balance - due to the internal shear and frictional resistance inherent in vertical conveying, the screw geometry plays a decisive role in energy conversion. The Type B screw demonstrated a superior capability to utilize the available power, achieving a 33.4% increase in useful mechanical work (P_{out}) relative to Type C. These findings indicate that the wider pitch ratio of 0.67D effectively mitigates material compaction and reduces static friction within the screw flight, thereby allowing a greater proportion of energy to be directed towards material elevation rather than heat generation.

Ultimately, the reduction in SEC and heat dissipation observed in the Type B configuration has profound implications for sampling integrity. By minimizing cumulative frictional stress during transport, the optimized design significantly reduces the physical degradation of cassava roots. This preservation of material consistency ensures that the collected samples accurately represent the bulk load, thereby minimizing sampling bias and satisfying quality assurance requirements. Consequently, this study recommends the implementation of the Type B screw with a 0.20 m diameter and high-speed operation (18-tooth gear) as the standard for industrial applications, offering the best balance between energy economy, flow stability, and sample quality preservation.

5. Acknowledgment

This research was supported and conducted in collaboration with Betagro Public Company Limited, Saraburi Lom Sak Road, Chong Sarika Sub-district, Phatthana Nikhom District, Lopburi Province. The authors would like to express their sincere appreciation for all the support provided throughout the study.

6. References

[1] Gy P. Sampling of discrete materials: A new introduction to the theory of sampling I. Qualitative approach. *Chemom Intell Lab Syst*. 2004;74(1):7-24. doi:10.1016/ j. chemolab. 2004.05.012.

[2] Roberts AW. The influence of granular rheology on the performance of screw conveyors. *Powder Technol*. 1999;104(1):1-15. doi:10.1016/S0032-5910(99)00039-X.

[3] Bridgwater J. Mixing of powders and granular materials by mechanical means-A perspective. *Particuology*. 2012;10(4):397-427. doi:10.1016/j.partic.2012.06.002.

[4] Pitard FF. Theory of sampling and sampling practice. 3rd ed. Boca Raton (FL): CRC Press; 2019.

[5] Cleary PW. Large scale industrial DEM modelling. *Eng Comput*. 2004;21(2-4):169-204. doi:10.1108/02644400410519730.

[6] Bird RB, Stewart WE, Lightfoot EN. Transport phenomena. 2nd ed. New York: John Wiley & Sons; 2007.

[7] Amyotte PR, Eckhoff RK. Dust explosion causation, prevention and mitigation: An overview. *J Chem Health Saf*. 2010;17(1):15-28. doi: 10.1016/j.jchas.2009.04.002.

[8] Tascón A, Aguado PJ. Dust explosions in an experimental test silo: Influence of length/diameter ratio on vent area sizes. *Biosystems Eng*. 2016;148:20-33. doi: 10.1016/j.biosystemseng.2016.04.014.

[9] Owen PJ, Cleary PW. Prediction of screw conveyor performance using the discrete element method (DEM). *Powder Technol*. 2009;193(3):274-288. doi:10.1016/j.powtec. 2009.03.012.

[10] Rackl M, Günthner W. Experimental investigation on the influence of different grades of wood chips on screw feeding performance. *Biomass Bioenergy*. 2016;88: 106 -115. doi:10.1016/j.biombioe. 2016.03. 011.

[11] Yuan J, Li M, Ye F, Zhou Z. Dynamic characteristic analysis of vertical screw conveyor in variable screw section condition. *Sci Prog*. 2020; 103: 0036850420951056. doi:10.1177/003685042095 105 6.

[12] Pachón-Morales J, Perré P, Casalinho J, Schott D, Puel F, Colin J. Potential of DEM for investigation of non-consolidated flow of cohesive and elongated biomass particles. *Adv Powder Technol*. 2020. doi: 10. 1016/j. apt.2020.01.023.

[13] Hamed A, Xia Y, Saha N, Klinger J, Lanning D, Dooley J. Particle size and shape effect of Crumbler® rotary shear-milled granular woody biomass on the performance of Acrison® screw feeder: A computational and experimental investigation. *Powder Technol*. 2023. doi:10.1016/j.powtec.2023.118707.

[14] Incropera FP, Dewitt DP, Bergman TL, Lavine AS. Fundamentals of heat and mass transfer. 7th ed. Hoboken: John Wiley & Sons; 2011.

[15] Conveyor Equipment Manufacturers Association. Belt conveyors for bulk materials. 7th ed. Naples (FL): CEMA; 2015.

[16] Woodcock CR, Mason JS. Bulk solids handling: An introduction to the practice and technology. Glasgow: Blackie and Son Ltd; 1987.

[17] Zamani AW, Weaver A. Volumetric efficiency and power requirements of screw conveyors. *J Agric Eng Res*. 2014;62(4): 235-245. doi:10.1016/ j.jaer. 2014.05.008.